Distance Effect Correction on TLS Intensity Data Using Naturally Homogeneous Targets

Kai Tan and Xiaojun Cheng

***Abstract*— The intensity data recorded by a terrestrial laser scanner (TLS) are significantly influenced by the distance between the scanned point and the scanner center. In this letter, we propose a new method to estimate the TLS distance–intensity relationship by using naturally homogeneous targets (NHT). Since the original intensity data of the NHT are simultaneously influenced by the incidence angle and distance, the incidence angle effect is first eliminated to obtain a corrected intensity that merely depends on distance. Then, the distance–intensity relationship is derived by analyzing the incidence angle corrected intensity data of the NHT. Results indicate that compared with existing methods the proposed method is accurate and easily implementable. The coefficient of variation for the intensity data can be reduced by 52% after correction by the proposed method.**

***Index Terms*— Distance effect, incidence angle, intensity correction, terrestrial laser scanning.**

I. Introduction

THE intensity provided by terrestrial laser scanners (TLS) is a source of information closely associated with the reflectance properties of a scanned surface and can be used as a major or complementary data source in various applications [1]. However, the original intensity is influenced by a number of factors. Given that instrumental configurations are kept constant and atmospheric attenuation can be ignored, the TLS intensity data are predominantly influenced by target reflectance, distance (range), and incidence angle [2]–[5]. To derive target reflectance properties from the intensity data, the distance and incidence angle effects should be eliminated.

The incidence angle effect mainly depends on the target surface characteristics and can be corrected by some bidirectional reflectance distribution functions (BRDF) [3], [6]–[8]. By contrast, the distance effect is primarily related to the instrumental properties. The photodetector of TLS would internally take some measures to adjust the power/amplitude of the laser echo to ensure the optimization of range determination [4], [9]. The adjustment makes the distance effect to no longer follow the laser radar equation [6]. As a result, the TLS distance–intensity relationship is empirically estimated. Generally, to estimate the distance–intensity relationship some reference targets can be scanned from minimum to maximum distances of the adopted scanner in steps of a small interval at a constant incidence angle [2], [3], [9]–[11]. Then, a certain mathematical function (e.g., linear, polynomial, or exponential) can be adopted to approximately fit the relationship between the intensity and distance by analyzing these discrete measured data of the reference targets. However, these methods have some fatal demerits. For one thing, the data acquisition and processing work are very laborious and time-consuming. For example, the scanning range scale of a certain TLS is from 2 to 50 m. To obtain the distance–intensity relationship at this range interval with maximum possible details, a reference target can be scanned from 2 to 50 m in steps of a small interval (e.g., 0.5 m) at a constant incidence angle (e.g., 0°) in a laboratory. Thus, the total number of the scanning stations would be 96. For another, the change of the distance is discontinuous though the distance step is made as small as possible. The discrete data cannot accurately reflect the distance–intensity relationship. Some local sharp changes of the intensity with respect to the distance would be omitted.

In this letter, a new method is proposed to estimate the TLS distance–intensity relationship by using natural homogeneous targets (NHT). NHT refer to the targets in nature whose material and radiometric characteristics are basically the same over the entire surface, e.g., a cement/asphalt road, a soil/sandy/gravel land, or a marble/lime/wooden wall. Since the changes in the distances for the NHT are nearly continuous, the major contribution of this letter is that the distance–intensity relationship can be reflected and accurately estimated in detail. In addition, the scanned data of the NHT are obtained by only one scanning station. The data acquisition and processing work are greatly reduced in the proposed method.

II. Methodology

Considering that the instrumental configurations and atmospheric attenuation effect can typically be neglected, the intensity value obtained by a TLS system is mainly influenced by target reflectance, incidence angle, and distance according to the laser radar equation [6]. These three factors are independent of each other and the original intensity value (I) can be expressed as [2], [3]

$$I(\rho, \theta, d) = f_1(\rho) \cdot f_2(\theta) \cdot f_3(d) \tag{1}$$

Manuscript received January 13, 2019; revised March 15, 2019 and May 2, 2019; accepted June 3, 2019. Date of publication July 1, 2019; date of current version February 26, 2020. This work was supported in part by the Key Laboratory of Surveying and Mapping Science and Geospatial Information Technology of Ministry of Natural Resources under Grant 201916, in part by the State Key Laboratory of Estuarine and Coastal Research in East China Normal University under Grant 2017RCDW06 and Grant 2017TASK06, in part by the Ministry of Science and Technology of China under Grant 2017YFE0107400, and in part by the National Natural Science Foundation of China under Grant 41671449. *(Corresponding author: Kai Tan.)*

K. Tan is with the State Key Laboratory of Estuarine and Coastal Research, East China Normal University, Shanghai 200241, China (e-mail: ktan@sklec.ecnu.edu.cn).

X. Cheng is with the College of Surveying and Geo-Informatics, Tongji University, Shanghai 200092, China (e-mail: cxj@tongji.edu.cn).

Color versions of one or more of the figures in this letter are available online at http://ieeexplore.ieee.org.

Digital Object Identifier 10.1109/LGRS.2019.2922226

where f_1, f_2, and f_3 are the functions of target reflectance ρ, incidence angle θ, and distance d. According to the definition of TLS intensity correction [4], [9], the corrected intensity (I_c) should be equal or proportional to the target reflectance. I_c can be expressed as [2], [12]

$$I_c(\rho) = C_0 \cdot f_1(\rho) \tag{2}$$

where C_0 is a constant. To make the corrected intensity comparable with the original intensity in the numerical scale, C_0 can be defined as $C_0 = f_2(\theta_s) \cdot f_3(d_s)$ where θ_s and d_s correspond to the standard/reference incidence angle and distance, respectively [2]. $f_2(\theta_s)$ and $f_3(d_s)$ are two constants and θ_s and d_s can be arbitrarily defined.

Since some instrumental effects may mix with the incidence angle effect, both $f_2(\theta)$ and $f_3(d)$ are related to the instrumental mechanisms. Therefore, different functions can be used to substitute $f_2(\theta)$ and $f_3(d)$ for various TLS systems. According to the conclusion in [2], based on the Weierstrass approximation theorem, both $f_2(\theta)$ and $f_3(d)$ can be empirically approximated by a polynomial regardless of the internal details of the instrumental mechanisms, i.e., $f_2(\theta) = \sum_{i=0}^{N_2}(\alpha_i \theta^i)$ and $f_3(d) = \sum_{i=0}^{N_3}(\beta_i d^i)$ where N_2, α_i, N_3, and β_i are polynomial parameters. By dividing (1) and (2), the corrected intensity can be calculated by

$$I_c(\rho) = I(\rho, \theta, d) \cdot \frac{\sum_{i=0}^{N_2}\left(\alpha_i \theta_s^i\right)}{\sum_{i=0}^{N_2}(\alpha_i \theta^i)} \cdot \frac{\sum_{i=0}^{N_3}\left(\beta_i d_s^i\right)}{\sum_{i=0}^{N_3}(\beta_i d^i)}. \tag{3}$$

The incidence angle is the angle between the surface normal vector and the incident laser beam vector. The estimation of the surface normal vector is implemented by computing the best-fitting plane with the available data on the nearby neighborhood of each measured laser point. The distance is calculated using the 3-D geometric coordinates of the scanned point and scanner center. To estimate the polynomial parameters in (3), a monotonic relationship must be made between the recorded intensity and the distance or incidence angle. Usually, some reference targets can be scanned at various incidence angles from 0° to 90° in steps of several degrees at a constant distance in order to determine the incidence angle–intensity relationship (i.e., N_2 and α_i) [2], [3], [9], [11], [12]. Generally, the intensity decreases with an increase in the incidence angle. A step of several degrees (e.g., 5°) is sufficient to obtain an accurate incidence angle–intensity relationship. Therefore, the estimation of N_2 and α_i is not discussed in this letter. Similarly, to estimate the distance–intensity relationship (i.e., N_3 and β_i) some reference targets can be scanned at various distances in steps of several meters at a constant incidence angle [2], [3], [9], [11], [12]. However, the distance–intensity relationship is very complex for TLS. A step of several meters in the distance may overpass some local sharp changes between the distance and the intensity. In this letter, a new method is proposed to estimate the parameters for the distance–intensity relationship by using NHT. The principles are introduced as follows.

To obtain the relationship between distance and intensity, the reflectance and incidence angle should be constants or unchanged as shown in (1). However, the incidence angles of the NHT are distributed in the range from 0° to 90°. Therefore, the original intensity data of the NHT should first be corrected to a standard incidence angle to eliminate the incidence angle effect.

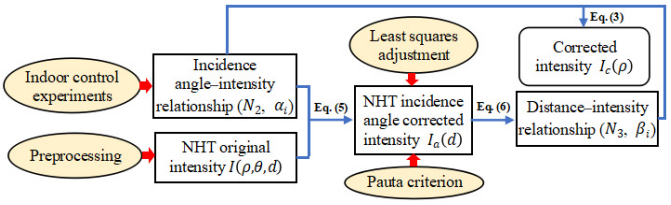

Fig. 1. Workflow of the proposed method.

Similar to (2), the incidence angle corrected intensity I_a related to the reflectance and distance can be expressed as [12]

$$I_a(\rho, d) = C_1 \cdot f_1(\rho) \cdot f_3(d) \tag{4}$$

where C_1 is a constant and can be defined as $C_1 = f_2(\theta_s)$. By dividing (4) and (1), I_a can be calculated by

$$I_a(\rho, d) = I(\rho, \theta, d) \cdot \frac{\sum_{i=0}^{N_2}\left(\alpha_i \theta_s^i\right)}{\sum_{i=0}^{N_2}(\alpha_i \theta^i)}. \tag{5}$$

For the NHT with reflectance ρ_y, ρ_y is unknown but constant. At this circumstance, the incidence angle corrected intensity I_a is merely related to the distance and $I_a(\rho, d)$ in (4) changed to $I_a(d)$. Equation (4) can be simplified as

$$I_a(d) = C \cdot \sum_{i=0}^{N_3}(\beta_i d^i) \tag{6}$$

where $C = f_1(\rho_y) \cdot f_2(\theta_s)$ is an unknown constant. First, N_3 can be determined by testing different orders of polynomials and comparing the fitting accuracy. Then, $K_i = C\beta_i$ can be estimated using a least squares adjustment of (6) by the data of the NHT. Thus, β_i can be calculated by $\beta_i = K_i / C$. Though the specific value of C is unknown, it does not influence the final intensity correction results. When substituting $\beta_i = K_i / C$ into (3), C is neutralized because C simultaneously exists in the numerators and denominators. Thus, K_i can be used to substitute β_i in the intensity correction. Since there are no ideal NHT, the Pauta criterion is adopted to preprocess the incidence angle corrected intensity data of the NHT to ensure good homogeneity and filter the outliers for an accurate estimation of K_i. If the residual $v = [\sum_{i=0}^{N_3}(K_i \cdot d^i) - I_a]$ of a certain point is three times larger than the standard deviation $\sigma_0 = (v^T v/(n - N_3 - 1))^{1/2}$ where n is the total number of points participating in the adjustment, this point is considered an outlier and is deleted. The rest points are then used to estimate K_i by conducting a least squares adjustment of (6) again.

After obtaining the parameters of K_i, the final corrected intensity can be calculated by (3). The overall workflow of the proposed method is illustrated in Fig. 1. Compared with the studies [2] and [12], the major innovation of this letter is that a new easily operational method instead of complicated indoor control experiments is proposed to accurately estimate N_3 and β_i by using NHT.

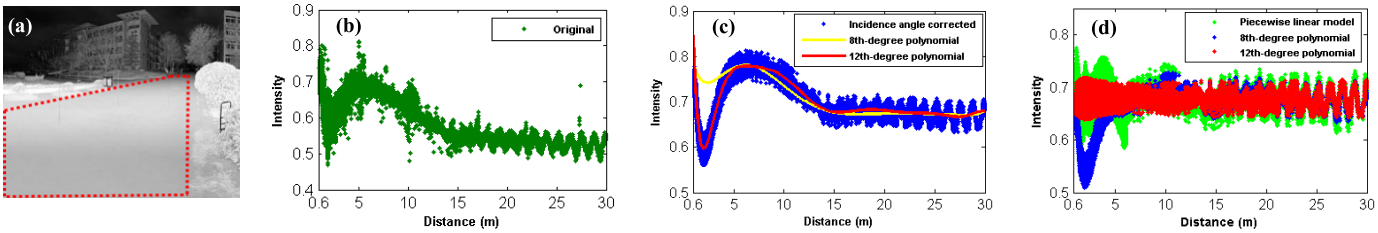

Fig. 2. (a) Original intensity image created by FARO SCENCE. Red dotted polygon: cement road. (b) Original intensity data (CV = 0.0718). Number of points: 325 808. (c) Incidence angle corrected intensity data and 8th-degree (indoor control experiments) and 12th-degree (NHT) polynomials. Number of points: 321 568. (d) Corrected intensity data by 8th-degree (CV = 0.0578) and 12th-degree (CV = 0.0151) polynomials and the PLM (CV = 0.0437).

III. Experiments and Results

The instrument adopted in this letter was Faro Focus^{3D} 120 (FARO Technologies, Inc., Orlando, FL, USA) which records intensity values in 11 bits [0, 2048]. The intensity values were normalized to [0, 1] for a direct comparison within and across different materials. Faro Focus^{3D} 120 can measure the distance from 0.6 to 120 m. The maximum distance is achieved under some specific conditions, e.g., perpendicular incidence angle, 90% target reflectance, and standard clear atmosphere. In actual scans, the maximum measured distance is considerably less than 120 m because the scanning environments can never meet all the specific conditions at which the maximum distance capability is achieved. In this letter, distances longer than 30 m were empirically disregarded to ensure good data reliability and quality of the point cloud [2], [12].

The polynomial parameters of $f_2(\theta)$ for Faro Focus^{3D} 120 were accurately estimated in our previous study [12]. In this letter, the incidence angle effect was not discussed in detail. The incidence angle effect was first eliminated by using the parameters in [12]. To derive the parameters of $f_3(d)$, a cement road in a campus was chosen [Fig. 2(a)]. The cement road was very long (width: 5 m) and the surface was basically homogeneous. Faro Focus^{3D} 120 was used to obtain the scanning data of the cement road. The data preprocessing work was conducted by the standard software FARO SCENE. The data analysis and algorithm programming were conducted in MATLAB. θ_s and d_s were defined as 0° and 15 m, respectively.

A total number of 325 808 points of the cement road with distances from 0.6 to 30 m were obtained. The original intensity with respect to distance for the cement road was shown in Fig. 2(b). It was worth noticing that a constant frequency oscillation occurred in the intensity data acquired at distances longer than 15 m. This may be due to the instrumental characteristics or the point density and did not have a significant influence on the overall trend of the intensity with respect to distance. Since there may be some dusts and surface damages, the cement road was not an ideal homogeneity. Some outliers existed in the intensity data as shown in Fig. 2(b). The incidence angle corrected intensity data were calculated by (5), and then the Pauta criterion was used to filter the outliers. The final incidence angle corrected intensity data of the cement road was shown in Fig. 2(c). Different orders of polynomials were tested and the values of σ_0 were compared. σ_0 significantly decreased from 1st- to the 12th-degrees polynomials. Later, σ_0 kept stable. Therefore, the 12th-degree polynomial was used to approximate $f_3(d)$ for Faro Focus^{3D} 120 by simultaneously considering the simplicity and accuracy of the polynomial fitting. By a least squares adjustment of (6) using the incidence angle corrected intensity data as shown in Fig. 2(c), the parameters K_i were obtained (Table I).

TABLE I
Parameters for K_i

K_0	K_1	K_2	K_3	K_4
4.44×10^{3}	-5.02×10^{3}	3.07×10^{3}	-9.82×10^{2}	1.92×10^{2}
K_5	K_6	K_7	K_8	K_9
-24.50	2.13	-0.13	5.30×10^{-3}	-1.49×10^{-4}
K_{10}	K_{11}	K_{12}		
2.71×10^{-6}	-2.88×10^{-8}	1.35×10^{-10}		

As shown in Fig. 2(c), the 12th-degree polynomial could accurately fit the incidence angle corrected intensity data from 0.6 to 30 m (the red curve). Also, the 8th-degree polynomial estimated by indoor control experiments in [10] was shown in Fig. 2(c) (the yellow curve). In [10], the distance was changed in steps of 1 m from 1 to 5 m and in steps of 2 m from 5 to 29 m. Thus, a total number of 17 stations were used to estimate N_3 and β_i. It can be seen that the 8th-degree polynomial approximately overlapped with the 12th-degree polynomial from 5 to 30 m. However, these two polynomials differed significantly from 0.6 to 5 m. This was because the distance effect of Faro Focus^{3D} 120 was very complicated from 0.6 to 5 m. The step of 1 m in [10] could not accurately reflect the sharp changes between distance and intensity at near distances. A total number of 17 stations could not perfectly depict the distance–intensity relationship. On the contrary, the distance–intensity relationship for Faro Focus^{3D} 120 was accurately estimated by scanning the cement road once. A total number of 321 437 points were included as shown in Fig. 2(c). This was equivalent to that 321 437 stations, set from 0.6 to 30 m. Thus, the distance–intensity relationship can be reflected in detail by using NHT.

The final corrected intensity data calculated by (3) were shown in Fig. 2(d). After correction by the 12th-degree polynomial, the intensity data acquired at different distances were approximately equal. The correction results by the 8th- and 12th-degrees polynomials were nearly the same from 5 to 30 m. However, the correction results of the 8th-degree polynomial were not satisfactory from 0.6 to 5 m since the 8th-degree polynomial could not well reflect the changes between distance and intensity at this interval. The coefficient of variation (CV), the ratio of the values

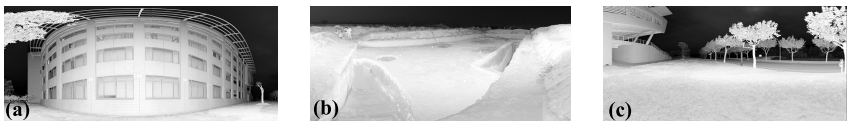

Fig. 3. Original intensity images created by FARO SCENCE. (a) Building. (b) Soil. (c) Lawn.

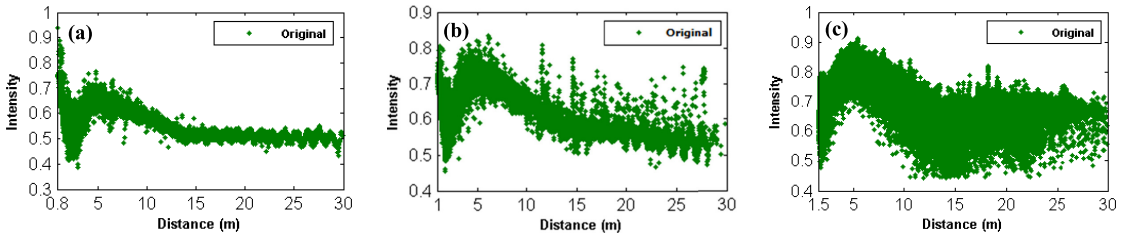

Fig. 4. Original intensity data with respect to distance. (a) Building. (b) Soil. (c) Lawn. The total number of points is 784 346, 569 210, and 465 249 for the building, soil, and lawn, respectively.

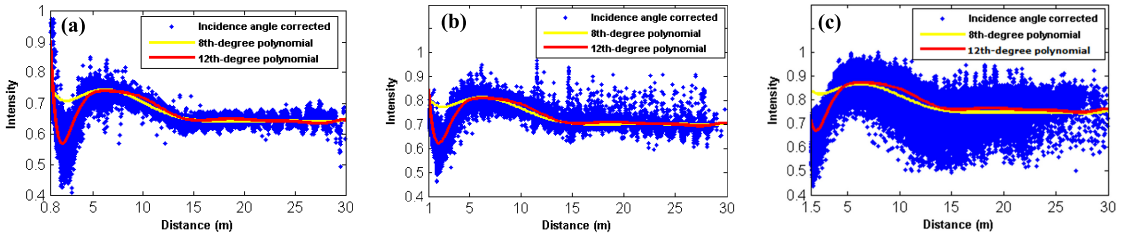

Fig. 5. Incidence angle corrected intensity data and 8th-degree (indoor control experiments) and 12th-degree (NHT) polynomials. (a) Building. (b) Soil. (c) Lawn.

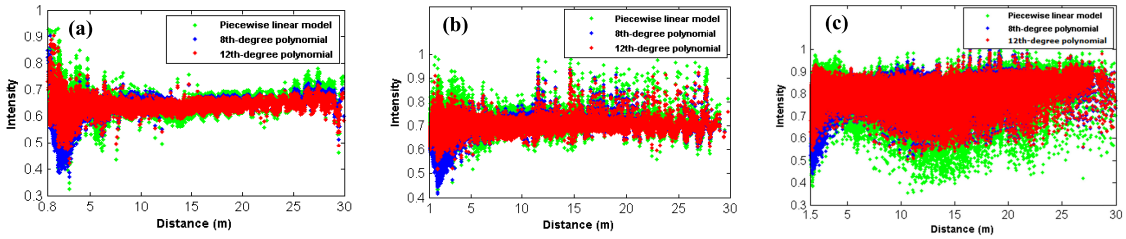

Fig. 6. Corrected intensity data by 8th-degree (indoor control experiments) and 12th-degree (NHT) polynomials and the PLM. (a) Building. (b) Soil. (c) Lawn.

of standard deviation to mean, was used to quantitatively evaluate the correction results [6]. CV was significantly reduced by 78.97% from 0.0718 for the original intensity data to 0.0151 for the corrected intensity data by the 12th-degree polynomial. On the contrary, CV were decreased only by 19.50% and 39.14% by the 8th-degree polynomial and the piecewise linear model (PLM) [10], respectively. The correction results suggested that with only one scanning campaign on an NHT, the proposed method can reflect the distance–intensity relationship with maximum possible details and can accurately estimate the polynomial parameters for distance effect correction.

IV. Validation and Discussion

A marble building facade, a soil pit, and an artificial lawn were scanned by Faro Focus^{3D} 120 to validate the feasibility and superiority of the proposed method (Fig. 3). The original and incidence angle corrected intensity data for the building (0.8–30 m), soil (1–30 m), and lawn (1.5–30 m) were shown in Figs. 4 and 5, respectively. Obviously, the 12th-degree polynomial estimated by the cement road in this letter overlapped well with the incidence angle corrected intensity data for the three targets. However, the 8th-degree polynomial still deviated significantly from the incidence angle corrected intensity data at distances below 5 m for the three targets.

The final corrected intensity data of the three targets using the parameters listed in Table I estimated by the cement road were shown in Fig. 6. Generally, the 12th-degree polynomial can accurately correct the distance effect. The correction results were very similar to that of the 8th-degree polynomial from 5 to 30 m. However, the correction results by the 8th-degree polynomial were unsatisfactory at distances below 5 m. It should be noted that the incidence angles of the lawn were difficult to reliably estimate because the grasses faced randomly to TLS and were usually smaller than the laser footprint. This led to the results that the corrected intensity data of the lawn acquired at the same distance differed slightly;

TABLE II
VALUES OF CV FOR DIFFERENT INTENSITY DATA

	Original	8th-/12th- degrees polynomial	PLM
Building	0.0544	0.0498/0.0318	0.0398
Soil	0.0793	0.0615/ 0.0226	0.0401
Lawn	0.0740	0.0643 /0.0438	0.0527

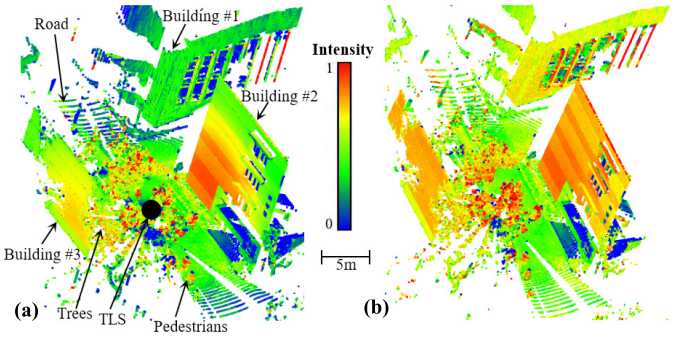

Fig. 7. Scene scanned by Faro Focus^{3D} 120. The total number of points is 453 584. (a) Point cloud colored by the incidence angle corrected data. The instrument was placed at the black solid circle. (b) Point cloud colored by the corrected intensity data of the proposed method.

hence, the intensity data in Fig. 6(c) are wider than that in Fig. 6(a) and (b). The values of CV for the original and corrected intensity data by different methods are listed in Table II. CV was reduced by approximately 52% for the three targets by the 12th-degree polynomial. On the contrary, the values of CV were averagely reduced by 14% and 35% by the eighth-degree polynomial and the PLM, respectively.

To further validate the feasibility of the proposed method visually, a scene scanned by Faro Focus^{3D} 120 was chosen (Fig. 7). The major targets in the scene included three buildings, a road, some trees, and some pedestrians. The intensity data of the buildings and road before and after distance effect correction were qualitatively compared. Due to the existence of the distance effect, the incidence angle corrected intensity data for different parts of the road differed drastically [Fig. 7(a)]. Also, the intensity data of the three buildings varied significantly. In particular, the intensity values of the upper part were totally different from that of the bottom part for Building #2. In addition, there was a big overlap in the intensity data of the road and Building #1 and Building #2. After correction by the 12th-degree polynomial in Table I, the differences in the intensity data from different part of the same target were greatly reduced [Fig. 7(b)]. For example, the corrected intensity data of the road at regions near and far away from the instrument were nearly equal. Also, the corrected intensity data of the three buildings were close. It became easy to distinguish the road and buildings using the corrected intensity data. The correction results indicated that the proposed method can accurately eliminate the distance effect on the intensity data and suggested that the corrected intensity data by the proposed method can be potentially used for point cloud classification and target feature extraction [13].

V. CONCLUSION

This letter proposes a new method to estimate the polynomial parameters for the distance effect correction on TLS intensity data using NHT. By merely scanning an NHT once, the polynomial parameters can be accurately estimated. Compared with the existing methods that adopt controlled experiments in indoor environments, this method is easy-operational and time-saving and can considerably reduce data acquisition and processing work. Additionally, the proposed method can reflect the distance–intensity relationship in detail and thus accurately eliminate the distance effect. The results indicate that the *CV* of the intensity data from a homogeneous target can be reduced by approximately 52%, which would greatly benefit the applications based on the intensity data. Another potential application of the proposed method is on the intensity data correction for long-distance TLS which can measure distance up to kilometers. Scanning reference targets from meters to kilometers is infeasible for long-distance TLS considering the length limit of indoor environments and the laborious data acquisition and processing work. Instead, using NHT could perfectly solve these problems for long-distance TLS. Theoretically, the proposed method can be popularized to other TLS. However, the applicability of the proposed method to other different TLS including long-distance ones should be further individually tested and validated.

REFERENCES

[1] J. U. H. Eitel *et al.*, "Beyond 3-D: The new spectrum of LiDAR applications for earth and ecological sciences," *Remote Sens. Environ.*, vol. 186, pp. 372–392, Dec. 2016.
[2] K. Tan and X. Cheng, "Intensity data correction based on incidence angle and distance for terrestrial laser scanner," *J. Appl. Remote Sens.*, vol. 9, Sep. 2015, Art. no. 094094.
[3] T. Xu, L. Xu, B. Yang, X. Li, and J. Yao, "Terrestrial laser scanning intensity correction by piecewise fitting and overlap-driven adjustment," *Remote Sens.*, vol. 9, no. 11, p. 1090, Oct. 2017.
[4] S. Kaasalainen, A. Krooks, A. Kukko, and H. Kaartinen, "Radiometric calibration of terrestrial laser scanners with external reference targets," *Remote Sens.*, vol. 1, pp. 144–158, 2009.
[5] A. F. C. Errington and B. L. F. Daku, "Temperature compensation for radiometric correction of terrestrial LiDAR intensity data," *Remote Sens.*, vol. 9, no. 4, p. 356, 2017.
[6] B. Höfle and N. Pfeifer, "Correction of laser scanning intensity data: Data and model-driven approaches," *ISPRS J. Photogramm. Remote Sens.*, vol. 62, no. 6, pp. 415–433, Dec. 2007.
[7] D. Carrea, A. Abellan, F. Humair, B. Matasci, M.-H. Derron, and M. Jaboyedoff, "Correction of terrestrial LiDAR intensity channel using Oren–Nayar reflectance model: An application to lithological differentiation," *ISPRS J. Photogramm. Remote Sens.*, vol. 113, pp. 17–29, Mar. 2016.
[8] Q. Ding, W. Chen, B. King, Y. Liu, and G. Liu, "Combination of overlap-driven adjustment and Phong model for LiDAR intensity correction," *ISPRS J. Photogram. Remote Sens.*, vol. 75, pp. 40–47, Jan. 2013.
[9] S. Kaasalainen, A. Jaakkola, M. Kaasalainen, A. Krooks, and A. Kukko, "Analysis of incidence angle and distance effects on terrestrial laser scanner intensity: Search for correction methods," *Remote Sens.*, vol. 3, no. 10, pp. 2207–2221, 2011.
[10] K. Tan, X. Cheng, X. Ding, and Q. Zhang, "Intensity data correction for the distance effect in terrestrial laser scanners," *IEEE J. Sel. Topics Appl. Earth Observ. Remote Sens.*, vol. 9, no. 1, pp. 304–312, Jan. 2016.
[11] W. Fang, X. Huang, F. Zhang, and D. Li, "Intensity correction of terrestrial laser scanning data by estimating laser transmission function," *IEEE Trans. Geosci. Remote Sens.*, vol. 53, no. 2, pp. 942–951, Feb. 2015.
[12] K. Tan and X. Cheng, "Correction of incidence angle and distance effects on TLS intensity data based on reference targets," *Remote Sens.*, vol. 8, no. 3, p. 251, 2016.
[13] Q. Li and X. Cheng, "Comparison of different feature sets for TLS point cloud classification," *Sensors*, vol. 18, no. 12, p. 4206, 2018.